Available online at www.sciencedirect.com
ScienceDirect
Journal of Hazardous Materials 144 (2007) 328–333
Journal of Hazardous Materials
www.elsevier.com/locate/jhazmat

Synthesis, characterization, and photocatalytic activity of $TiO_{2-x}N_x$ nanocatalyst

Y.Q. Wang [a,*], X.J. Yu [a,b,**], D.Z. Sun [a]

[a] School of Municipal and Environmental Engineering, Harbin Institute of Technology, Harbin, Heilongjiang 150090, PR China
[b] Department of Environmental Science and Engineering, Heilongjiang University, Harbin, Heilongjiang 150080, PR China

Received 21 April 2006; received in revised form 10 October 2006; accepted 11 October 2006
Available online 15 October 2006

Abstract

Nitrogen-doped titanium dioxide powders were prepared by wet method, that is, the hydrolysis of acidic tetra-butyl titanate using aqueous ammonia solution, followed by calcination at temperatures about 350 °C. The catalysts exhibited photocatalytic activity in the visible light region owing to N-doping. The light absorption onset of $TiO_{2-x}N_x$ was shifted to the visible region at 459 nm compared to 330 nm of pure TiO_2. An obvious decrease in the band gap was observed by the optical absorption spectroscopy, which resulted from N2p localized states above the valence band of $TiO_{2-x}N_x$ (compared to TiO_2). The $TiO_{2-x}N_x$ catalyst was characterized to be anatase with oxygen-deficient stoichiometry by X-ray diffraction (XRD), surface photovoltage spectroscopy (SPS) and X-ray photoelectron spectroscopy (XPS). The binding energy of N1s measured by XPS characterization was 396.6 eV (Ti─N bonds, β-N) and 400.9 eV (N─N bonds, γ-N_2), respectively. The photocatalytic activity of $TiO_{2-x}N_x$ under visible light was induced by the formation of β-N in the structure. Photocatalytic decomposition of benzoic acid solutions was carried out in the ultraviolet and visible (UV–vis) light region, and the $TiO_{2-x}N_x$ catalyst showed higher activity than pure TiO_2.
© 2006 Elsevier B.V. All rights reserved.

Keywords: Photocatalyst; Visible light; Wet method; N-doped TiO_2; Benzoic acid

1. Introduction

Semiconductor-based photocatalysis, as an effective means of alleviating very low concentrations of pollutants including airborne pathogenic microorganisms, viruses, and volatile organic contaminants, has attracted extensive interests [1–5], after the discovery of the photoinduced decomposition of water on TiO_2 reported by Fujishima and Honda [6]. It is well known that titanium dioxide was the most effective photocatalyst and was widely applied in the purification of air and water, solar system. However, most of these investigations were carried out under ultraviolet (UV) light, because TiO_2 photocatalyst showed relatively high activity and chemical stability under UV light ($\lambda \leq 387.5$ nm). Nevertheless, solar energy contains only about 5% UV light and the rest is visible light. In order to utilize sunlight or rays from artificial sources more effectively in photocatalytic reaction, the development of photocatalysts showing high activity under visible light irradiation is needed. For this purpose, coupling with organic dye sensitizers or metal oxides [7–9], doping of TiO_2 with transition metals [10,11] and reduced forms of TiO_x photocatalysts [12] have been investigated. However, most of these catalysts do not show long-term stability or do not have sufficiently high photocatalytic activities for a wide range of applications. Asahi et al. [13] reported that N-doped TiO_2 showed photoabsorption at wavelengths longer than 400 nm. They have also reported that the N-doped TiO_2 has photocatalytic activity under visible light during the photodegradation of acetaldehyde and methylene blue. Then, some researchers prepared the N-doped TiO_2 and obtained many results [14–17]. At present, the N-doped TiO_2 films or powders are prepared by: (1) sputtering TiO_2 targets for several hours in an N_2/Ar gas mixture and then annealing in N_2 gas [13], (2) treating anatase TiO_2 powders in an NH_3/Ar atmosphere to produce photocatalysts [14,15], and (3) a hydrolytic process using a $TiCl_3$ or $Ti(SO_4)_2$ solution and an ammonia solution [16,17].

The previous researches have proved that photocatalytic activity is strongly related to the crystallinity, particle size and specific surface area of the photocatalyst [18–20]. Although

* Corresponding author. Tel.: +86 451 822 91642.
** Corresponding author. Tel.: +86 451 864 13259.
E-mail addresses: biguiwang@163.com (Y.Q. Wang), yuxjuan@hit.edu.cn (X.J. Yu).

0304-3894/$ – see front matter © 2006 Elsevier B.V. All rights reserved.
doi:10.1016/j.jhazmat.2006.10.033

three of the TiO_2 polymorphs, rutile, anatase and brookite occur in nature, usually, only anatase and rutile can be utilized as photocatalysts. The photocatalytic activity of brookite has been seldom investigated. Both anatase and rutile can be described in terms of distorted TiO_6 octahedra, that is, Ti^{4+} ions surrounded by six O^{2-} ions. The rutile structure has a slight orthorhombic distortion, while the anatase octahedron is more distorted. Moreover, anatase has greater Ti–Ti distances than rutile (3.79 and 3.04 Å versus 3.57 and 2.96 Å), but shorter Ti–O distances (1.934 and 1.980 Å versus 1.949 and 1.980 Å) [21]. The different structures result in different electronic band properties. The band gap of anatase is 3.2 eV [22], while that of rutile is slightly smaller at 3.0 eV [23]. So, anatase is usually considered to be more active than rutile crystalline form in photocatalytic research.

Under these circumstances, we demonstrated a simple hydrolysis method of nitrogen-doped TiO_2 ($TiO_{2-x}N_x$) using tetra-butyl titanate as titanium source. The new method avoided the laborious process compared to the traditional hydrolysis methods using inorganic titanium sources that need washing off residual SO_4^{2-} and Cl^- [16,17]. The experiment results indicated that the $TiO_{2-x}N_x$ prepared here has highly visible light-induced photocatalytic activity for degradation of benzoic acid solutions. Moreover, the phase composition, particle size, microstructure, specific surface area and photoelectrochemical properties of the $TiO_{2-x}N_x$ were determined by X-ray diffraction (XRD), Brauenner–Emmet–Teller (BET), surface photovoltage spectroscopy (SPS), electric-field-induced surface photovoltage spectroscopy (EFISPS) and X-ray photoelectron spectroscopy (XPS) analyses.

2. Experimental

2.1. Preparation of $TiO_{2-x}N_x$

Tetra-butyl titanate ($Ti(OBu)_4$) solution was used as a titanium stock. Ammonia aqueous solution ($NH_3{\cdot}H_2O$) (25%) was used as a nitrogen source. Under stirring, 0.5 mL nitric acid (HNO_3) was added drop wise into a solution mixed with 20 mL $Ti(OBu)_4$ and 100 mL ethanol at room temperature. Here, HNO_3 was used as a chemical additive to moderate the reaction rate, in order to control the reaction kinetics. Then, 40 mL $NH_3{\cdot}H_2O$ was added dropwise under stirring to carry out hydrolysis. After continuously stirring for 60 min, the precursor was dried in an oven at 80 °C. Finally, the precursor was calcined at 350 °C for 1 h to obtain the $TiO_{2-x}N_x$. The color of the sample powder was grey. The $Ti(OBu)_4$ and $NH_3{\cdot}H_2O$ were obtained from Shanghai Reagent Co., China. At the same time, the pure TiO_2 was prepared by sol–gel [24] in order to compare with $TiO_{2-x}N_x$.

2.2. Analytical method

The crystal phases of the sample were analyzed by X-ray diffraction with Cu Kα radiation (XRD: model D/max-rB, Rigaku Co., Tokyo, Japan). The particles were spread on a glass slide specimen holder and the scattered intensity was measured between 10 and 90 °C at a scanning rate of $2\theta = 5$ °C/min with 0.02 °C increments. Nitrogen adsorption and desorption isotherms were collected at −196 °C on a quantachrome autosorb-1 sorption analyzer. The specific surface area was calculated using the BET model. The SPS instrument was assembled at Heilongjiang University, and monochromatic light was obtained by passing light from a 500 W xenon lamp (CHF-XQ500W, China) through a double prism monochromator (SBP300, China). A lock-in amplifer (SR830, USA), synchronized with a light chopper (SR540, USA), was employed to amplify the photovoltage signal. The powder sample was sandwiched between two ITO glass electrodes. The UV–vis absorption spectra of the samples were recoded on a spectrophotometer (UV-3100, Shimadzu Co., Kyoto, Japan). The absorption percentage (A) was obtained by measuring the transmittance (T) and reflectance (R) of the powders, where $A = 100 - (T + R)$. A 60 mm-integrating sphere was used for the measurement, since the scattering effect was taken into account for the powders absorption. X-ray photoelectron spectroscopy with Al Kα X-rays (XPS: model PHI5700 ESCA, Physical Electronics USA) was used to evaluate the amount and states of the nitrogen atoms in these powders. All binding energies (BE) were calibrated by the BE (284.6 eV) of C1s, which gave BE values within an accuracy of ±0.1 eV.

2.3. Photocatalytic oxidation of benzoic acid under simulated sunlight

The photocatalytic activity of the prepared catalyst was estimated by decomposition of 25 mg L^{-1} benzoic acid (BA) using 0.1 g L^{-1} of photocatalyst dosage. The photoreactor consisted of a cylindrical borosilicate glass reactor, a cooling water jacket and a light source from a 125 W Xe lamp (Institute of Electric Light Source, Beijing) located axially at the center of the vessel. The effective volume of the photoreactor was 1250 mL. The Xe lamp usually was used as simulated sunlight because the energy distribution of the Xe lamp was identical to sunlight [25]. The photocatalyst powder was added directly into the air-bubbling benzoic acid solutions followed by ultrasonic dispersion for 20 min before irradiation. The solutions were kept at 25 °C by cooling water. A special glass atmolyzer as air diffuser was fixed at the bottom of the reactor to uniformly disperse air into the solution. After irradiation, the solution was filtered through a 0.45 μm membrane filter. The concentration of benzoic acid was determined by total organic carbon (TOC) measurements using TOC-V_{CPN} (Shimadzu).

2.4. The comparison of activity between $TiO_{2-x}N_x$ and TiO_2 under different irradiation wavelength

The photocatalytic activity of $TiO_{2-x}N_x$ and TiO_2 catalysts was estimated by measuring the decomposition rate of benzoic acid (25 mg L^{-1}) within 2-h reaction time, in which contains 60 mg of photocatalyst and 60 mL of benzoic acid solution. Ultrasonic was first used to disperse the photocatalyst in solution and a magnetic stirrer was used to mix the solution during the reaction. A 125 W Xe lamp was used to photo-irradiate the suspension. Different irradiation wavelengths were obtained by

Table 1
Structural property of the photocatalyst samples

Sample	Anatase (%)	Crystallite size (nm)	BET surface area ($m^2\ g^{-1}$)	Micropore volume ($cc\ g^{-1}$)	Average pore size (Å)
TiO_2	81	8	114.3	0.2186	76.50
$TiO_{2-x}N_x$	100	9	139.3	0.2827	81.18

passing through a series of ZWB2, ZWB3, DTB500 or DTB600 filter (Nantong Xiangyang Optical Element Co. Ltd., China), the corresponding main irradiation wavelengths were 365, 334, 500 and 600 nm, respectively. The benzoic acid concentrations were measured by HPLC (LC-10A System, Shimadzu, Japan) equipped with a TSK-GEL ODS C18 column. A mixture of aqueous solution (92% NaH_2PO_4: 50 mmol L^{-1}; 5% methanol; 3% acetic acid) was used as an eluent.

3. Results and discussion

3.1. The X-ray diffraction and Brauenner–Emmet–Teller analysis

The crystalline phase of $TiO_{2-x}N_x$ and TiO_2 was analyzed by XRD, and the XRD results are shown in Fig. 1. X-ray structure analysis for the $TiO_{2-x}N_x$ obtained at 350 °C calcination showed that the characteristic peaks of anatase were observed and the peaks of rutile and dopant-related were not detected. The dopants may have moved into either the interstitial positions or the substitutional sites of the TiO_2 crystal structure [26]. The polycrystalline anatase structure was further confirmed by (1 0 1), (0 0 4), (2 0 0), (1 0 5), and (2 1 1) diffraction peaks. Its tetragonal Bravais lattic-type was also testified by lattice constant calculated from these peaks. It could therefore be concluded that the $TiO_{2-x}N_x$ obtained at 350 °C calcination was the anatase TiO_2-based polycrystalline powder. But the pure TiO_2 obtained at 350 °C calcination was measured to be composed of 81% anatase and 19% rutile. The transition from anatase to rutile during the preparation of $TiO_{2-x}N_x$ was restrained by the doping of N in the lattice. Therefore, the conclusion could be attained that the $TiO_{2-x}N_x$ had higher photocatalytic activity than pure TiO_2 because the band gap of anatase was higher than the rutile one [22,23]. Sato et al. [27] analyzed their N-doped TiO_2 with XRD and observed that the crystal form of doped samples calcined at temperatures below 500 °C was also anatase. Mwabora et al. [28] have also reported that the presence of nitrogen seemed to induce a rutile to anatase transition for the TiO_2-like structure.

The effective grain size D of samples was estimated by the Scherrer's equation, that is, $D = 0.98\lambda/(\beta \cos(2\theta))$, where λ is the X-ray wavelength of the Cu Kα radiation applied ($\lambda = 1.5405$ Å), β is the full-width at half maximum intensity of the diffraction peak and θ is the Bragg's angle of diffraction. At the same time, the phase composition was calculated from quantitative formula [29]: $x = (1 + 0.8\, I_A/I_R)^{-1}$, where x is the weight fraction of rutile in the sample, I_A and I_R are the X-ray intensities of the anatase and the rutile peaks, respectively. The Scherrer crystallite sizes, lattice parameter, and other characteristics were given (Table 1). Both the TiO_2 and $TiO_{2-x}N_x$ were nanoparticles, and the doping of N did not show any significant effect on the crystallite size of the catalysts. Both of them could appear quantum size effect under the illumination [30]. The BET analysis showed that the specific surface area, pore volume and pore diameter of $TiO_{2-x}N_x$ were larger than pure TiO_2 due to the addition of N, and $TiO_{2-x}N_x$ had higher photocatalytic activity than pure TiO_2.

3.2. The surface photovoltage spectroscopy and diffuse reflectance spectra analysis

Fig. 2 showed the SPS spectra of $TiO_{2-x}N_x$ and TiO_2. It could be seen that the TiO_2 had a broad absorption band from 300 to 400 nm due to the transition of the O^{2-} antibonding orbital to the lowest empty orbital of Ti^{4+}, but the absorption band of $TiO_{2-x}N_x$ was shifted to 400–525 nm. According to the results

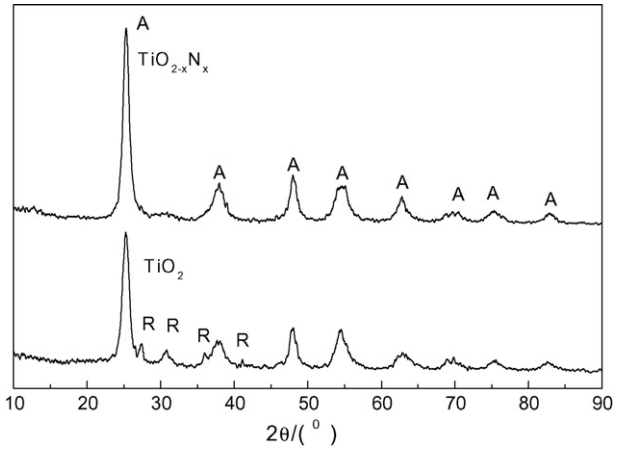

Fig. 1. XRD pattern of $TiO_{2-x}N_x$ and TiO_2 (A—anatase, R—rutile).

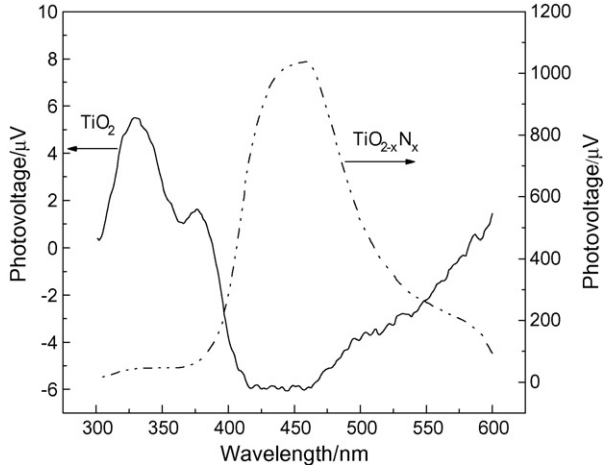

Fig. 2. SPS spectra of $TiO_{2-x}N_x$ and TiO_2.

of XRD, the absorption band of $TiO_{2-x}N_x$ should exhibit the blue shift because the band gap of anatase TiO_2 (3.2 eV) is higher than the band gap of rutile TiO_2 (3.0 eV). On the contrary, $TiO_{2-x}N_x$ obviously exhibited red shift, and the maximum responsive signal was at 459 nm according to the SPS spectra. This phenomenon could be analyzed by the theory of density of states, the band gap of $TiO_{2-x}N_x$ was reduced and the separation efficiency of electron and hole was increased by N modification. The corresponding band gap of $TiO_{2-x}N_x$ was 2.7 eV calculated from formula [31]: $E_g = 1240/\lambda$ (eV) (here $\lambda = 459$ nm). Irie et al. [15] have previously reported the optical absorption properties and quantum yield values for nitrogen doped TiO_2 powders and concluded that the isolated narrow band of N2p orbitals formed above the valence band was responsible for the visible light activity.

Fig. 3 showed the EFISPS spectra of the $TiO_{2-x}N_x$. The remarkable changes of SPS response of $TiO_{2-x}N_x$ could be observed when an external electric field was applied. As shown in Fig. 3, higher photovoltage could be achieved under higher positive external electric field; on the contrary, when an opposite external electric field was employed, the response became weaker, which was common characteristic of n-type semiconductors. When the experiment was performed under a positive bias, the SPS response exhibited mainly two obvious features. One was the increase of SPS response, which could be explained by the fact that the direction of external electric field was in accord with that of built-in electric field of the $TiO_{2-x}N_x$. The other feature was that the strong SPS response was broadened, which was attributed to the trap-to-band transitions [32]. The electron-trapped surface states may result from surface oxygen vacancies and hydroxyl [33].

The diffuse reflectance spectra (DRS) of $TiO_{2-x}N_x$ and TiO_2 calcined at 350 °C were shown in Fig. 4 The inset in Fig. 4 showed that the optical absorption edge (in eV) and band gap of $TiO_{2-x}N_x$ calcined at 350 °C became narrowed compared to pure TiO_2. It can be seen from Fig. 4 that the visible light absorption of $TiO_{2-x}N_x$ was extended to 600 nm compared to pure TiO_2. The inset in Fig. 4 also showed a clear-cut shift in the optical absorption edge toward the visible region on $TiO_{2-x}N_x$ compared to TiO_2, which indicated that the nitrogen species occupied some of the oxygen positions in the $TiO_{2-x}N_x$ lattice. This also ruled out the occupancy of N in any other positions such as interstitial sites, which should give rise to a mid-gap band between valence and conduction bands.

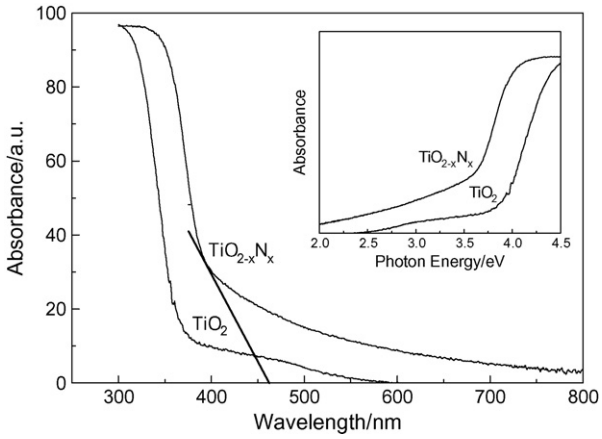

Fig. 4. Optical absorbance spectra of TiO_2 and $TiO_{2-x}N_x$.

3.3. The X-ray photoelectron spectroscopy analysis

The N atomic composition of $TiO_{2-x}N_x$ was analyzed with XPS. As shown in Fig. 5 two N1s XPS peaks were present at 400.9 and 396.6 eV, respectively. The results were in agreement with the reports [14,15]. Asahi et al. [14] assigned these two peaks as atomic β-N (396 eV, Ti–N bonds) and molecularly chemisorbed γ-N_2 (400 eV, N–N bonds). Next, they plotted the visible light photocatalytic activity of their N-doped TiO_2 against the ratio of β-N and the total N, and found the visible light photocatalytic activity increased linearly with the increase of β-N. From this result, they thought that the visible light sensitization of N-doped TiO_2 was ascribed to the formation of Ti–N bonding. Irie et al. [15] also prepared N-doped TiO_2 by a NH_3-treatment method and examined the relation between the amount of N doped and the photocatalytic activity for 2-propanol photooxidation under visible light as well as under

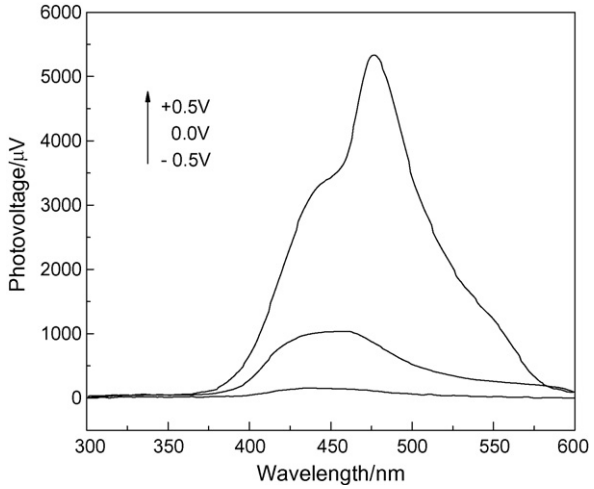

Fig. 3. EFISPS spectra of $TiO_{2-x}N_x$.

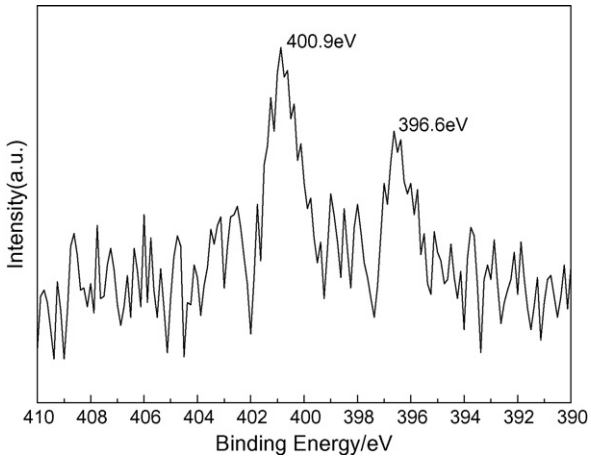

Fig. 5. N1s XPS spectra of $TiO_{2-x}N_x$.

UV. They observed N1s peak at 396 and 400 eV in XPS analysis and ascribed the 396 eV state to visible light sensitization. But the results of Diwald et al. [34] rather indicated negative contribution of Ti–N bonding to photocatalytic activity. So, the contribution of Ti–N bonding to the visible-light sensitization of TiO_2 remained in doubt. The chemical composition of $TiO_{2-x}N_x$ could be approximately calculated from the peak intensities of the XPS spectra by the relative sensitivity factor method. The x values could be determined by the ratio of the peaks areas at 396.6 eV and at 531.0 eV, which corresponded to O1s, Ti–O bonds. The composition of $TiO_{2-x}N_x$ in the present research was determined to be $TiO_{1.975}N_{0.025}$.

3.4. The photocatalytic experimental

Fig. 6 showed the TOC removal rate of photocatalytic decomposition of benzoic acid solutions by $TiO_{2-x}N_x$ and TiO_2, respectively. As shown in Fig. 6, 53.4% of TOC removal efficiency was achieved by $TiO_{2-x}N_x$ in 120-min reaction time, but for pure TiO_2 photocatalyst, only 21.6% was observed. Obviously, the photocatalytic activity was significantly improved by N-modification. This could be explained by the following hints, since the Xe lamp could be regarded as simulated sunlight, and the wavelength of the light was composed with UV–vis light. TiO_2 could only be excited under the illumination of the UV light ($\lambda \leq 387.5$ nm), but the $TiO_{2-x}N_x$ had photocatalytic activity under visible light ($\lambda \leq 459$ nm) due to the extension of adsorption region as shown in the analysis of SPS and DRS (seen in Figs. 2 and 4). Therefore, the photocatalytic activity of the $TiO_{2-x}N_x$ was superior to the pure TiO_2.

As shown in Fig. 7, the removal rate of benzoic acid increased with the increase of irradiation time. The photocatalytic activity of $TiO_{2-x}N_x$ was higher than TiO_2 for each wavelength tested in the experiments. When the wavelength of irradiation range was changed to visible region (for example 500 and 600 nm), the pure TiO_2 did not show any photocatalytic activity. But for $TiO_{2-x}N_x$, 4.6% of the removal rate of benzoic acid could be obtained under the irradiation of 600 nm light in 120-min reaction time. The results agreed with the analysis of SPS and DRS.

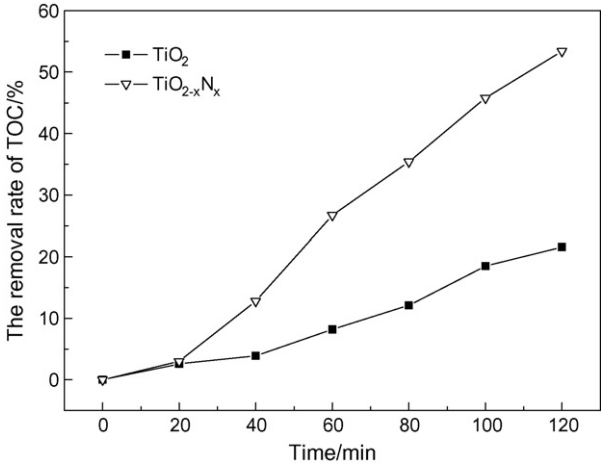

Fig. 6. TOC removal rate of $TiO_{2-x}N_x$ and TiO_2.

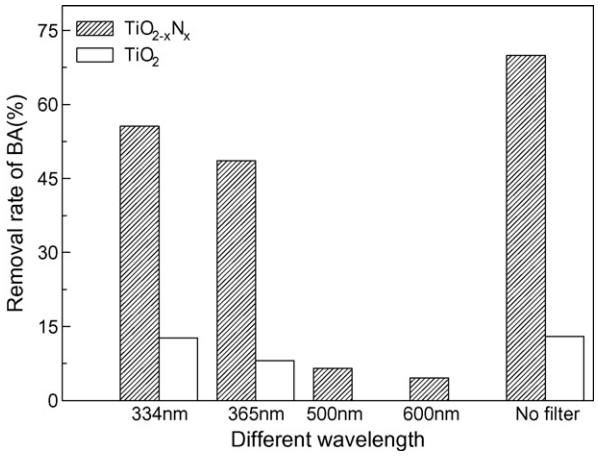

Fig. 7. Benzoic acid removal rate under different wavelength for $TiO_{2-x}N_x$ and TiO_2.

4. Conclusions

An anatase type of $TiO_{2-x}N_x$ nanophotocatalyst with a homogeneous size (9 nm) was prepared by a simple chemical route followed by calcination at temperatures about 350 °C. The presence of nitrogen could restrain an anatase to rutile transition for the catalyst according to XRD analysis. The light absorption onset of $TiO_{2-x}N_x$ in the visible-light region (400–525 nm) was clearly observed. The advantages of this method compared to other preparation methods were (1) use of inexpensive chemical precursors for the synthesis of $TiO_{2-x}N_x$ and (2) formation of $TiO_{2-x}N_x$ as uniformly sized nanoparticles. Optical absorption studies clearly identified the substitutional N-doping and localized N-states in the TiO_2 lattice. XPS results indicated that the status of N to be anion-like (N^-) and chemical environment of N was as in Ti–N bonding in the TiO_2 lattice. The binding energy of N1s of $TiO_{2-x}N_x$ was 400.9 and 396.6 eV. The photocatalytic activity of $TiO_{2-x}N_x$ under visible light was related to the peak intensity of β-N atoms at 396.6 eV, and the composition was determined to be $TiO_{1.975}N_{0.025}$ by the relative sensitivity factor method. The photocatalytic decomposition of benzoic acid under simulated sunlight and visible region showed that $TiO_{2-x}N_x$ catalyst had higher photocatalytic activity than pure TiO_2 in the decomposition.

Acknowledgements

This project is supported by the National Natural Science Foundation of China (No. 50378027). Special thanks are extended to the department of Chemistry, Heilongjiang University, China, for allowing us the use of the SPS and DRS facilities.

References

[1] T. Nuida, N. Kanai, K. Hashimoto, T. Watanabe, H. Ohsaki, Enhancement of photocatalytic activity using UV light trapping effect, Vacuum 74 (2004) 729.

[2] P.B. Amama, K. Itoh, M. Murabayashi, Gas-phase photocatalytic degradation of trichloroethylene on pretreated TiO_2, Appl. Catal. B-Environ. 37 (2002) 321.

[3] R. Wang, K. Hashimoto, A. Fujishima, M. Chikuni, E. Kojima, A. Kitamura, M. Shimohigoshi, T. Watanabe, Light-induced amphiphilic surfaces, Nature 388 (1997) 431.
[4] X.C. Wang, J.C. Yu, C. Ho, Y. Hou, X. Fu, Photocatalytic activity of a hierarchically macro/mesoporous titania, Langmuir 21 (2005) 2552.
[5] M.R. Hoffmann, S.T. Martin, W. Choi, D.W. Bahnemann, Environmental applications of semiconductor photocatalysis, Chem. Rev. 95 (1995) 69.
[6] A. Fujishima, K. Honda, Electronchemical photolysis of water at a semiconductor electrode, Nature 238 (1972) 37.
[7] M.G. Kang, N.G. Park, Y.J. Park, K.S. Ryu, S.H. Chang, Manufacturing method for transparent electric windows using dye-sensitized TiO_2 solar cells, Sol. Energy Mater. Sol. Cells 75 (2003) 475.
[8] K.B. Dhanalakshmi, S. Latha, S. Anadan, P. Maruthamuthu, Dye sensitized hydrogen evolution from water, Int. J. Hydrogen Energy 26 (2001) 669.
[9] C.C. Bandara, W.G. Hadapangoda, Jayasekera, TiO_2/MgO composite photocatalyst: the role of MgO in photoinduced charge carrier separation, Appl. Catal. B-Environ. 50 (2004) 83.
[10] U. Siemon, D. Bahnemann, J.J. Testa, D. Rodríguez, M.I. Litter, N. Bruno, Degradation of propanol diluted in water under visible light irradiation using metal ion-implanted titanium dioxide photocatalysts, J. Photochem. Photobiol. A-Chem. 148 (2002) 247.
[11] A. Yamakata, T.A. Ishibashi, H. Onishi, Effects of accumulated electrons on the decay kinetics of photogenerated electrons in Pt/TiO_2 photocatalyst studied by time-resolved infrared absorption spectroscopy, J. Photochem. Photobiol. A-Chem. 160 (2003) 33.
[12] I. Nakamura, N. Negishi, S. Kutsuna, T. Ihara, S. Sugihara, K. Takeuchi, Role of oxygen vacancy in the plasma-treated TiO_2 photocatalyst with visible light activity for NO removal, J. Mol. Catal. A-Chem. 161 (2000) 205.
[13] R. Asahi, T. Morikawa, T. Ohwaki, K. Aoki, Y. Taga, Visible-light photocatalysis in nitrogen-doped titanium oxides, Science 293 (2001) 269.
[14] M. Miyauchi, A. Ikezawa, H. Tobimatsu, K. Hashimoto, Zeta potential and photocatalytic activity of nitrogen doped TiO_2 thin film, Phys. Chem. Chem. Phys. 6 (2004) 865.
[15] H. Irie, Y. Watanabe, K. Hashimoto, Nitrogen-concentration dependence on photocatalytic activity of $TiO_{2-x}N_x$ powders, J. Phys. Chem. B 107 (2003) 5483.
[16] T. Ihara, M. Miyoshi, Y. Iriyama, O. Matsumoto, S. Sugihara, Visible-light-active titanium oxide photocatalyst realized by an oxygen-deficient structure and by nitrogen doping, Appl. Catal. B-Environ. 42 (2003) 403.
[17] A.V. Voronsov, A.A. Altynnikov, E.N. Savinov, E.N. Kurkin, Correlation of TiO_2 photocatalytic activity and diffuse reflectance spectra, J. Photochem. Photobiol. A-Chem. 144 (2001) 193.
[18] L. Kavan, M. Gratzel, S.E. Gilbert, C. Klemenz, H.J. Scheel, Electrochemical and photoelectrochemical investigation of single-crystal anatase, J. Am. Chem. Soc. 118 (1996) 6716.
[19] M. Toyoda, Y. Nanbu, Y. Nakazawa, M. Hirano, M. Inagaki, Effect of crystallinity of anatase on photoactivity for methyleneblue decomposition in water, Appl. Catal. B-Environ. 49 (2004) 227.
[20] E. Beyers, P. Cool, E.F. Vansant, Anatase formation during the synthesis of mesoporous titania and its photocatalytic effect, J. Phys. Chem. B 109 (2005) 10081.
[21] A.L. Linsebigler, G.Q. Lu, J.T. Yates, Photocatalysis on TiO_2 surfaces: principles, mechanisms, and selected results, Chem. Rev. 95 (1995) 735.
[22] H. Tang, H. Berger, P.E. Schmid, F. Lévy, G. Burri, Photoluminescence in TiO_2 anatase single crystals, Solid State Commun. 87 (1993) 847.
[23] J. Pascual, J. Camassel, H. Mathieu, Fine structure in the intrinsic absorption edge of TiO_2, Phys. Rev. B 18 (1978) 5606.
[24] D.Z. Sun, S. Chen, S.C. Jong, X.D. Duan, Z.B. Zhu, Photocatalytic degradation of toluene using a novel flow reactor with Fe-doped TiO_2 catalyst on porous nickel sheets, Photochem. Photobiol. 81 (2005) 352.
[25] Y.Q. Wang, X.J. Yu, H.F. Yang, Q. Ming, D.Z. Sun, Preparation and characterization of visible-light responsive photocatalyst S/TiO_2, Chin. J. Inorg. Chem. 22 (2006) 771.
[26] Z.P. Wang, W.M. Cai, X.T. Hong, X.L. Zhao, F. Xu, C.G. Cai, Photocatalytic degradation of phenol in aqueous nitrogen-doped TiO_2 suspensions with various light sources, Appl. Catal. B-Environ. 57 (2005) 223.
[27] S. Sato, R. Nakamura, S. Abe, Visible-light sensitization of TiO_2 photocatalysts by wet-method N-doping, Appl. Catal. A-Gen. 284 (2005) 131.
[28] J.M. Mwabora, T. Lindgren, E. Avendano, T.F. Jaramillo, J. Lu, S.E. Lindquist, C.G. Granqvist, Structure, composition, and morphology of photoelectrochemically active $TiO_{2-x}N_x$ thin films deposited by reactive DC magnetron sputtering, J. Phys. Chem. B 108 (2004) 20193.
[29] R.A. Spurr, H. Myers, Quantitative analysis of anatase–rutile mixtures with an X-ray diffractometer, Anal. Chem. 29 (1957) 760.
[30] M.I. Litter, J.A. Navío, Photocatalytic properties of iron-doped titania semiconductors, J. Photochem. Photobiol. A-Chem. 98 (1996) 171.
[31] A. Hagfeldt, M. Graetzel, Light-induced redox reactions in nanocrystalline systems, Chem. Rev. 95 (1995) 49.
[32] X.M. Qian, D.Q. Qin, Q. Song, Y.B. Bai, T.J. Li, X.Y. Tang, E.K. Wang, S.J. Dong, Surface photovoltage spectra and photoelectrochemical properties of semiconductor-sensitized nanostructured TiO_2 electrodes, Thin Solid Films 385 (2001) 152.
[33] L.Q. Jing, X.J. Sun, J. Shang, W.M. Cai, Z.L. Xu, Y.G. Du, H.G. Fu, Review of surface photovoltage spectra of nano-sized semiconductor and its applications in heterogeneous photocatalysis, Sol. Energy Mater. Sol. Cells 79 (2003) 133.
[34] O. Diwald, T.L. Thompson, E.G. Goralski, S.D. Walck, J.T. Yates, The effect of nitrogen ion implantation on the photoactivity of TiO_2 rutile single crystals, J. Phys. Chem. B 108 (2004) 52.